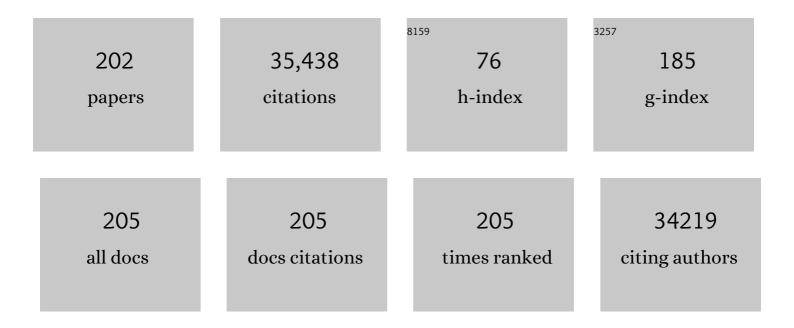
## Xinran Wang

List of Publications by Year in descending order

Source: https://exaly.com/author-pdf/4299034/publications.pdf Version: 2024-02-01



#	Article	IF	CITATIONS
1	Chemically Derived, Ultrasmooth Graphene Nanoribbon Semiconductors. Science, 2008, 319, 1229-1232.	6.0	4,504
2	Narrow graphene nanoribbons from carbon nanotubes. Nature, 2009, 458, 877-880.	13.7	2,313
3	N-Doping of Graphene Through Electrothermal Reactions with Ammonia. Science, 2009, 324, 768-771.	6.0	2,020
4	Highly conducting graphene sheets and Langmuir–Blodgett films. Nature Nanotechnology, 2008, 3, 538-542.	15.6	1,901
5	Room-Temperature All-Semiconducting Sub-10-nm Graphene Nanoribbon Field-Effect Transistors. Physical Review Letters, 2008, 100, 206803.	2.9	1,345
6	Highly anisotropic and robust excitons in monolayer black phosphorus. Nature Nanotechnology, 2015, 10, 517-521.	15.6	1,204
7	Strong Photoluminescence Enhancement of MoS <sub>2</sub> through Defect Engineering and Oxygen Bonding. ACS Nano, 2014, 8, 5738-5745.	7.3	995
8	Hopping transport through defect-induced localized states in molybdenum disulphide. Nature Communications, 2013, 4, 2642.	5.8	935
9	Facile synthesis of high-quality graphene nanoribbons. Nature Nanotechnology, 2010, 5, 321-325.	15.6	757
10	High-responsivity graphene/silicon-heterostructure waveguide photodetectors. Nature Photonics, 2013, 7, 888-891.	15.6	731
11	Atomic Layer Deposition of Metal Oxides on Pristine and Functionalized Graphene. Journal of the American Chemical Society, 2008, 130, 8152-8153.	6.6	623
12	Towards intrinsic charge transport in monolayer molybdenum disulfide by defect and interface engineering. Nature Communications, 2014, 5, 5290.	5.8	563
13	Bandgap engineering of two-dimensional semiconductor materials. Npj 2D Materials and Applications, 2020, 4, .	3.9	528
14	Electrical characterization of back-gated bi-layer MoS2 field-effect transistors and the effect of ambient on their performances. Applied Physics Letters, 2012, 100, .	1.5	515
15	Integrated digital inverters based on two-dimensional anisotropic ReS2 field-effect transistors. Nature Communications, 2015, 6, 6991.	5.8	505
16	Highâ€Electronâ€Mobility and Airâ€Stable 2D Layered PtSe <sub>2</sub> FETs. Advanced Materials, 2017, 29, 1604230.	11.1	502
17	Selective Etching of Metallic Carbon Nanotubes by Gas-Phase Reaction. Science, 2006, 314, 974-977.	6.0	489
18	Graphene and related two-dimensional materials: Structure-property relationships for electronics and optoelectronics. Applied Physics Reviews, 2017, 4, .	5.5	476

#	Article	IF	CITATIONS
19	Etching and narrowing of graphene from the edges. Nature Chemistry, 2010, 2, 661-665.	6.6	441
20	Room temperature high-detectivity mid-infrared photodetectors based on black arsenic phosphorus. Science Advances, 2017, 3, e1700589.	4.7	419
21	Layer-by-Layer Thinning of MoS <sub>2</sub> by Plasma. ACS Nano, 2013, 7, 4202-4209.	7.3	387
22	A Selfâ€Healable, Highly Stretchable, and Solution Processable Conductive Polymer Composite for Ultrasensitive Strain and Pressure Sensing. Advanced Functional Materials, 2018, 28, 1705551.	7.8	387
23	Langmuirâ^'Blodgett Assembly of Densely Aligned Single-Walled Carbon Nanotubes from Bulk Materials. Journal of the American Chemical Society, 2007, 129, 4890-4891.	6.6	373
24	Silicon CMOS devices beyond scaling. IBM Journal of Research and Development, 2006, 50, 339-361.	3.2	352
25	Epitaxial growth of wafer-scale molybdenum disulfide semiconductor single crystals on sapphire. Nature Nanotechnology, 2021, 16, 1201-1207.	15.6	339
26	A MoS <sub>2</sub> /PTCDA Hybrid Heterojunction Synapse with Efficient Photoelectric Dual Modulation and Versatility. Advanced Materials, 2019, 31, e1806227.	11.1	336
27	Protein microarrays with carbon nanotubes as multicolor Raman labels. Nature Biotechnology, 2008, 26, 1285-1292.	9.4	317
28	Two-dimensional quasi-freestanding molecular crystals for high-performance organic field-effect transistors. Nature Communications, 2014, 5, 5162.	5.8	315
29	Black Phosphorus Radio-Frequency Transistors. Nano Letters, 2014, 14, 6424-6429.	4.5	307
30	Analyzing the Carrier Mobility in Transitionâ€Metal Dichalcogenide MoS <sub>2</sub> Fieldâ€Effect Transistors. Advanced Functional Materials, 2017, 27, 1604093.	7.8	265
31	Planar carbon nanotube–graphene hybrid films for high-performance broadband photodetectors. Nature Communications, 2015, 6, 8589.	5.8	258
32	Top–down fabrication of sub-nanometre semiconducting nanoribbons derived from molybdenum disulfide sheets. Nature Communications, 2013, 4, 1776.	5.8	220
33	Probing Carrier Transport and Structure-Property Relationship of Highly Ordered Organic Semiconductors at the Two-Dimensional Limit. Physical Review Letters, 2016, 116, 016602.	2.9	220
34	Highâ€Performance Monolayer WS <sub>2</sub> Fieldâ€Effect Transistors on Highâ€₽̂ Dielectrics. Advanced Materials, 2015, 27, 5230-5234.	11.1	218
35	Realization of Roomâ€Temperature Phononâ€Limited Carrier Transport in Monolayer MoS <sub>2</sub> by Dielectric and Carrier Screening. Advanced Materials, 2016, 28, 547-552.	11.1	218
36	A self-powered high-performance graphene/silicon ultraviolet photodetector with ultra-shallow junction: breaking the limit of silicon?. Npj 2D Materials and Applications, 2017, 1, .	3.9	211

#	Article	IF	CITATIONS
37	Uniform and ultrathin high-κ gate dielectrics for two-dimensional electronic devices. Nature Electronics, 2019, 2, 563-571.	13.1	204
38	Stacked 2D materials shed light. Nature Materials, 2015, 14, 264-265.	13.3	203
39	Gate-tunable van der Waals heterostructure for reconfigurable neural network vision sensor. Science Advances, 2020, 6, eaba6173.	4.7	202
40	Graphene nanoribbons with smooth edges behave as quantum wires. Nature Nanotechnology, 2011, 6, 563-567.	15.6	197
41	Stretchable elastic synaptic transistors for neurologically integrated soft engineering systems. Science Advances, 2019, 5, eaax4961.	4.7	191
42	Thermally Limited Current Carrying Ability of Graphene Nanoribbons. Physical Review Letters, 2011, 106, 256801.	2.9	190
43	DNA Functionalization of Carbon Nanotubes for Ultrathin Atomic Layer Deposition of High κ Dielectrics for Nanotube Transistors with 60 mV/Decade Switching. Journal of the American Chemical Society, 2006, 128, 3518-3519.	6.6	188
44	A light-stimulated synaptic device based on graphene hybrid phototransistor. 2D Materials, 2017, 4, 035022.	2.0	186
45	Uniform nucleation and epitaxy of bilayer molybdenum disulfide on sapphire. Nature, 2022, 605, 69-75.	13.7	174
46	Graphene Nanoribbons from Unzipped Carbon Nanotubes: Atomic Structures, Raman Spectroscopy, and Electrical Properties. Journal of the American Chemical Society, 2011, 133, 10394-10397.	6.6	170
47	Electrically driven thermal light emission from individual single-walled carbon nanotubes. Nature Nanotechnology, 2007, 2, 33-38.	15.6	167
48	Programmable transition metal dichalcogenide homojunctions controlled by nonvolatile ferroelectric domains. Nature Electronics, 2020, 3, 43-50.	13.1	167
49	Hydrogenation and Hydrocarbonation and Etching of Single-Walled Carbon Nanotubes. Journal of the American Chemical Society, 2006, 128, 6026-6027.	6.6	159
50	Design strategies for twoâ€dimensional material photodetectors to enhance device performance. InformaÄnÃ-Materiály, 2019, 1, 33-53.	8.5	158
51	Ultrahigh mobility and efficient charge injection in monolayer organic thin-film transistors on boron nitride. Science Advances, 2017, 3, e1701186.	4.7	146
52	Defect Engineering for Modulating the Trap States in 2D Photoconductors. Advanced Materials, 2018, 30, e1804332.	11.1	146
53	Graphene nanoribbons for quantum electronics. Nature Reviews Physics, 2021, 3, 791-802.	11.9	141
54	2D Singleâ€Crystalline Molecular Semiconductors with Precise Layer Definition Achieved by Floatingâ€Coffeeâ€Ringâ€Driven Assembly. Advanced Functional Materials, 2016, 26, 3191-3198.	7.8	136

#	Article	IF	CITATIONS
55	Novel Field-Effect Schottky Barrier Transistors Based on Graphene-MoS2 Heterojunctions. Scientific Reports, 2014, 4, 5951.	1.6	134
56	Epitaxial Ultrathin Organic Crystals on Graphene for Highâ€Efficiency Phototransistors. Advanced Materials, 2016, 28, 5200-5205.	11.1	134
57	Graphene Hybrid Structures for Integrated and Flexible Optoelectronics. Advanced Materials, 2020, 32, e1902039.	11.1	127
58	Defects as a factor limiting carrier mobility in WSe2: A spectroscopic investigation. Nano Research, 2016, 9, 3622-3631.	5.8	126
59	Three-dimensional monolithic micro-LED display driven by atomically thin transistor matrix. Nature Nanotechnology, 2021, 16, 1231-1236.	15.6	120
60	MoTe <sub>2</sub> p–n Homojunctions Defined by Ferroelectric Polarization. Advanced Materials, 2020, 32, e1907937.	11.1	115
61	Biaxial Compressive Strain Engineering in Graphene/Boron Nitride Heterostructures. Scientific Reports, 2012, 2, 893.	1.6	113
62	A spectrally tunable all-graphene-based flexible field-effect light-emitting device. Nature Communications, 2015, 6, 7767.	5.8	113
63	Assessment of Chemically Separated Carbon Nanotubes for Nanoelectronics. Journal of the American Chemical Society, 2008, 130, 2686-2691.	6.6	111
64	Sensitive and Ultrabroadband Phototransistor Based on Twoâ€Dimensional Bi <sub>2</sub> O <sub>2</sub> Se Nanosheets. Advanced Functional Materials, 2019, 29, 1905806.	7.8	106
65	Metal-Enhanced Fluorescence of Carbon Nanotubes. Journal of the American Chemical Society, 2010, 132, 15920-15923.	6.6	105
66	Graphene/Organic Semiconductor Heterojunction Phototransistors with Broadband and Biâ€directional Photoresponse. Advanced Materials, 2018, 30, e1804020.	11.1	103
67	Highâ€Performance Graphene Devices on SiO <sub>2</sub> /Si Substrate Modified by Highly Ordered Selfâ€Assembled Monolayers. Advanced Materials, 2011, 23, 2464-2468.	11.1	101
68	Band Gap Opening of Bilayer Graphene by F4-TCNQ Molecular Doping and Externally Applied Electric Field. Journal of Physical Chemistry B, 2010, 114, 11377-11381.	1.2	98
69	200 GHz Maximum Oscillation Frequency in CVD Graphene Radio Frequency Transistors. ACS Applied Materials & Interfaces, 2016, 8, 25645-25649.	4.0	97
70	Quantitative Analysis of Graphene Doping by Organic Molecular Charge Transfer. Journal of Physical Chemistry C, 2011, 115, 7596-7602.	1.5	94
71	Angle-selective perfect absorption with two-dimensional materials. Light: Science and Applications, 2016, 5, e16052-e16052.	7.7	94
72	Precise, Self-Limited Epitaxy of Ultrathin Organic Semiconductors and Heterojunctions Tailored by van der Waals Interactions. Nano Letters, 2016, 16, 3754-3759.	4.5	92

#	Article	IF	CITATIONS
73	Embedded Ag quantum dots into interconnected Co3O4 nanosheets grown on 3D graphene networks for high stable and flexible supercapacitors. Electrochimica Acta, 2017, 224, 260-268.	2.6	89
74	Ultra-Low-Power Smart Electronic Nose System Based on Three-Dimensional Tin Oxide Nanotube Arrays. ACS Nano, 2018, 12, 6079-6088.	7.3	88
75	Improving the Performance of Graphene Phototransistors Using a Heterostructure as the Light-Absorbing Layer. Nano Letters, 2017, 17, 6391-6396.	4.5	87
76	Sub-thermionic, ultra-high-gain organic transistors and circuits. Nature Communications, 2021, 12, 1928.	5.8	83
77	Chemical self-assembly of graphene sheets. Nano Research, 2009, 2, 336-342.	5.8	80
78	Efficient and Layerâ€Dependent Exciton Pumping across Atomically Thin Organic–Inorganic Typeâ€I Heterostructures. Advanced Materials, 2018, 30, e1803986.	11.1	79
79	Band Structure Engineering of Interfacial Semiconductors Based on Atomically Thin Lead Iodide Crystals. Advanced Materials, 2019, 31, e1806562.	11.1	79
80	A van der Waals pn heterojunction with organic/inorganic semiconductors. Applied Physics Letters, 2015, 107, 183103.	1.5	77
81	Mesoporous iron oxide directly anchored on a graphene matrix for lithium-ion battery anodes with enhanced strain accommodation. RSC Advances, 2013, 3, 699-703.	1.7	76
82	ZnO-nanorods/graphene heterostructure: a direct electron transfer glucose biosensor. Scientific Reports, 2016, 6, 32327.	1.6	76
83	Tunable Plasmon–Phonon Polaritons in Layered Graphene–Hexagonal Boron Nitride Heterostructures. ACS Photonics, 2015, 2, 907-912.	3.2	70
84	Graphene charge-injection photodetectors. Nature Electronics, 2022, 5, 281-288.	13.1	70
85	Tunable, Ultralowâ€Power Switching in Memristive Devices Enabled by a Heterogeneous Graphene–Oxide Interface. Advanced Materials, 2014, 26, 3275-3281.	11.1	69
86	Mo-O bond doping and related-defect assisted enhancement of photoluminescence in monolayer MoS <sub>2</sub> . AIP Advances, 2014, 4, 123004.	0.6	69
87	Three-Dimensional Topological Insulator Bi <sub>2</sub> Te <sub>3</sub> /Organic Thin Film Heterojunction Photodetector with Fast and Wideband Response from 450 to 3500 Nanometers. ACS Nano, 2019, 13, 755-763.	7.3	68
88	A scalable sulfuration of WS2 to improve cyclability and capability of lithium-ion batteries. Nano Research, 2016, 9, 857-865.	5.8	67
89	Optical Characterizations and Electronic Devices of Nearly Pure (10,5) Single-Walled Carbon Nanotubes. Journal of the American Chemical Society, 2009, 131, 2454-2455.	6.6	63
90	. Edge magnetotransport fingerprints in disordered graphene nanoribbons. Physical Review B, 2010, 82,	1.1	63

#	Article	IF	CITATIONS
91	Interfacial amplification for graphene-based position-sensitive-detectors. Light: Science and Applications, 2017, 6, e17113-e17113.	7.7	62
92	High-Performance Black Phosphorus Field-Effect Transistors with Long-Term Air Stability. Nano Letters, 2019, 19, 331-337.	4.5	62
93	Evidence of weak localization in quantum interference effects observed in epitaxial La0.7Sr0.3MnO3 ultrathin films. Scientific Reports, 2016, 6, 26081.	1.6	61
94	Topological transport and atomic tunnelling–clustering dynamics for aged Cu-doped Bi2Te3 crystals. Nature Communications, 2014, 5, 5022.	5.8	60
95	Strong optical response and light emission from a monolayer molecular crystal. Nature Communications, 2019, 10, 5589.	5.8	59
96	Lowâ€Power Complementary Inverter with Negative Capacitance 2D Semiconductor Transistors. Advanced Functional Materials, 2020, 30, 2003859.	7.8	58
97	Roomâ€Temperature Edge Functionalization and Doping of Graphene by Mild Plasma. Small, 2011, 7, 574-577.	5.2	56
98	Solvothermal Synthesis of Lateral Heterojunction Sb <sub>2</sub> Te <sub>3</sub> /Bi <sub>2</sub> Te <sub>3</sub> Nanoplates. Nano Letters, 2015, 15, 5905-5911.	4.5	56
99	Solventâ€Based Softâ€Patterning of Graphene Lateral Heterostructures for Broadband High‧peed Metal–Semiconductor–Metal Photodetectors. Advanced Materials Technologies, 2017, 2, 1600241.	3.0	53
100	Layerâ€Defining Strategy to Grow Twoâ€Dimensional Molecular Crystals on a Liquid Surface down to the Monolayer Limit. Angewandte Chemie - International Edition, 2019, 58, 16082-16086.	7.2	53
101	Solutionâ€Processed 2D Molecular Crystals: Fabrication Techniques, Transistor Applications, and Physics. Advanced Materials Technologies, 2019, 4, 1800182.	3.0	53
102	Speed up Ferroelectric Organic Transistor Memories by Using Two-Dimensional Molecular Crystalline Semiconductors. ACS Applied Materials & Interfaces, 2017, 9, 18127-18133.	4.0	52
103	Oxide Synaptic Transistors Coupled With Triboelectric Nanogenerators for Bio-Inspired Tactile Sensing Application. IEEE Electron Device Letters, 2020, 41, 617-620.	2.2	51
104	Ultrahigh Stability 3D TI Bi <sub>2</sub> Se <sub>3</sub> /MoO <sub>3</sub> Thin Film Heterojunction Infrared Photodetector at Optical Communication Waveband. Advanced Functional Materials, 2020, 30, 1909659.	7.8	50
105	Sensitive and Robust Ultraviolet Photodetector Array Based on Self-Assembled Graphene/C <sub>60</sub> Hybrid Films. ACS Applied Materials & Interfaces, 2018, 10, 38326-38333.	4.0	48
106	Doubling the Power Output of Bifacial Thinâ€Film GaAs Solar Cells by Embedding Them in Luminescent Waveguides. Advanced Energy Materials, 2013, 3, 991-996.	10.2	47
107	The positive piezoconductive effect in graphene. Nature Communications, 2015, 6, 8119.	5.8	43
108	Carrier scattering in graphene nanoribbon field-effect transistors. Applied Physics Letters, 2008, 92, .	1.5	40

#	Article	IF	CITATIONS
109	Light-modulated vertical heterojunction phototransistors with distinct logical photocurrents. Light: Science and Applications, 2020, 9, 167.	7.7	40
110	Retinaâ€Inspired Selfâ€Powered Artificial Optoelectronic Synapses with Selective Detection in Organic Asymmetric Heterojunctions. Advanced Science, 2022, 9, e2103494.	5.6	40
111	Coherent and Tunable Terahertz Radiation from Graphene Surface Plasmon Polarirons Excited by Cyclotron Electron Beam. Scientific Reports, 2015, 5, 16059.	1.6	39
112	Experimental evidence and control of the bulk-mediated intersurface coupling in topological insulator <mml:math xmlns:mml="http://www.w3.org/1998/Math/MathML"&gt;<mml:mrow><mml:msub><mml:mi>Bi</mml:mi><mm Physical Review B, 2015, 91, .</mm </mml:msub></mml:mrow></mml:math 	l:mn> <sup>121</sup> /mn	nl:mn>
113	ZrO <sub>2</sub> Ferroelectric FET for Non-volatile Memory Application. IEEE Electron Device Letters, 2019, 40, 1419-1422.	2.2	38
114	Spin-Coated Crystalline Molecular Monolayers for Performance Enhancement in Organic Field-Effect Transistors. Journal of Physical Chemistry Letters, 2018, 9, 1318-1323.	2.1	37
115	Low-defect-density WS2 by hydroxide vapor phase deposition. Nature Communications, 2022, 13, .	5.8	37
116	Repairing atomic vacancies in single-layer MoSe2 field-effect transistor and its defect dynamics. Npj Quantum Materials, 2017, 2, .	1.8	36
117	Epitaxial Topological Insulator Bi <sub>2</sub> Te <sub>3</sub> for Fast Visible to Mid-Infrared Heterojunction Photodetector by Graphene As Charge Collection Medium. ACS Nano, 2022, 16, 4851-4860.	7.3	35
118	Tuning the transport behavior of centimeter-scale WTe2 ultrathin films fabricated by pulsed laser deposition. Applied Physics Letters, 2017, 111, .	1.5	34
119	Precise Extraction of Charge Carrier Mobility for Organic Transistors. Advanced Functional Materials, 2020, 30, 1904508.	7.8	34
120	Field-effect transistors based on two-dimensional materials for logic applications. Chinese Physics B, 2013, 22, 098505.	0.7	32
121	Low-voltage, High-performance Organic Field-Effect Transistors Based on 2D Crystalline Molecular Semiconductors. Scientific Reports, 2017, 7, 7830.	1.6	32
122	Two dimensional WS2 lateral heterojunctions by strain modulation. Applied Physics Letters, 2016, 108, 263104.	1.5	31
123	Synthesis, charge transport and device applications of graphene nanoribbons. Synthetic Metals, 2015, 210, 109-122.	2.1	30
124	Realization of vertical and lateral van der Waals heterojunctions using two-dimensional layered organic semiconductors. Nano Research, 2017, 10, 1336-1344.	5.8	30
125	Negative capacitance 2D MoS <inf>2</inf> transistors with sub-60mV/dec subthreshold swing over 6 orders, 250 l1/4A/l1/4m current density, and nearly-hysteresis-free. , 2017, , .		30
126	pJ-Level Energy-Consuming, Low-Voltage Ferroelectric Organic Field-Effect Transistor Memories. Journal of Physical Chemistry Letters, 2019, 10, 2335-2340.	2.1	30

#	Article	IF	CITATIONS
127	Planar graphene-C60-graphene heterostructures for sensitive UV-Visible photodetection. Carbon, 2019, 146, 486-490.	5.4	30
128	Soft hydrogen plasma induced phase transition in monolayer and few-layer MoTe <sub>2</sub> . Nanotechnology, 2019, 30, 034004.	1.3	29
129	Electronic Properties of Graphene Altered by Substrate Surface Chemistry and Externally Applied Electric Field. Journal of Physical Chemistry C, 2012, 116, 6259-6267.	1.5	28
130	Graphene integrated photodetectors and opto-electronic devices — a review. Chinese Physics B, 2017, 26, 034203.	0.7	27
131	Directly writing 2D organic semiconducting crystals for high-performance field-effect transistors. Journal of Materials Chemistry C, 2017, 5, 11246-11251.	2.7	27
132	Tailoring exciton dynamics of monolayer transition metal dichalcogenides by interfacial electron-phonon coupling. Communications Physics, 2019, 2, .	2.0	27
133	Intrinsic p-type W-based transition metal dichalcogenide by substitutional Ta-doping. Applied Physics Letters, 2017, 111, .	1.5	26
134	Room-temperature photoconduction assisted by hot-carriers in graphene for sub-terahertz detection. Carbon, 2018, 130, 233-240.	5.4	26
135	Uniform wurtzite MnSe nanocrystals with surface-dependent magnetic behavior. Nano Research, 2013, 6, 275-285.	5.8	25
136	Organic charge-transfer interface enhanced graphene hybrid phototransistors. Organic Electronics, 2019, 64, 22-26.	1.4	25
137	Fewâ€Layer Organic Crystalline van der Waals Heterojunctions for Ultrafast UV Phototransistors. Advanced Electronic Materials, 2020, 6, 2000062.	2.6	22
138	Soft and transient magnesium plasmonics for environmental and biomedical sensing. Nano Research, 2018, 11, 4390-4400.	5.8	21
139	Nanocrystal-Embedded-Insulator (NEI) Ferroelectric Field-Effect Transistor Featuring Low Operating Voltages and Improved Synaptic Behavior. IEEE Electron Device Letters, 2019, 40, 1933-1936.	2.2	20
140	Polarimetric Three-Dimensional Topological Insulators/Organics Thin Film Heterojunction Photodetectors. ACS Nano, 2019, 13, 10810-10817.	7.3	20
141	Large-area uniform few-layer PtS2: Synthesis, structure and physical properties. Materials Today Physics, 2021, 18, 100376.	2.9	20
142	Flexible field-effect transistor arrays with patterned solution-processed organic crystals. AIP Advances, 2013, 3, .	0.6	19
143	Tailored Plasmons in Pentacene/Graphene Heterostructures with Interlayer Electron Transfer. Nano Letters, 2019, 19, 6058-6064.	4.5	19
144	Electrically driven light emission from hot single-walled carbon nanotubes at various temperatures and ambient pressures. Applied Physics Letters, 2007, 91, .	1.5	18

#	Article	IF	CITATIONS
145	A ternary composite with manganese dioxide nanorods and graphene nanoribbons embedded in a polyaniline matrix for high-performance supercapacitors. RSC Advances, 2017, 7, 33591-33599.	1.7	18
146	Interfacial Flat-Lying Molecular Monolayers for Performance Enhancement in Organic Field-Effect Transistors. ACS Applied Materials & Interfaces, 2018, 10, 22513-22519.	4.0	18
147	Ferroelectric tunnel junctions with high tunnelling electroresistance. Nature Electronics, 2020, 3, 440-441.	13.1	18
148	Fabrication Techniques of Graphene Nanostructures. RSC Nanoscience and Nanotechnology, 2014, , 1-30.	0.2	17
149	A molecular understanding of the gas-phase reduction and doping of graphene oxide. Nano Research, 2012, 5, 361-368.	5.8	16
150	Highâ€Performance Flexible Allâ€Solidâ€State Supercapacitors Based on Ultralarge Graphene Nanosheets and Solventâ€Exfoliated Tungsten Disulfide Nanoflakes. Advanced Materials Interfaces, 2017, 4, 1700419.	1.9	16
151	Ultraâ€Narrowband Photodetector with High Responsivity Enabled by Integrating Monolayer Jâ€Aggregate Organic Crystal with Graphene. Advanced Optical Materials, 2021, 9, 2100158.	3.6	15
152	Carbon Nanotubes: From Growth, Placement and Assembly Control to 60mV/decade and Sub-60 mV/decade Tunnel Transistors. , 2006, , .		14
153	Unveiling the piezoelectric nature of polar α-phase P(VDF-TrFE) at quasi-two-dimensional limit. Scientific Reports, 2018, 8, 532.	1.6	14
154	Photoresponsivity of an all-semimetal heterostructure based on graphene and WTe2. Scientific Reports, 2018, 8, 12840.	1.6	14
155	Room-temperature observations of the weak localization in low-mobility graphene films. Journal of Applied Physics, 2013, 114, 214502.	1.1	13
156	Unveiling the structural origin of the high carrier mobility of a molecular monolayer on boron nitride. Physical Review B, 2014, 90, .	1.1	13
157	Large [6,6]-phenyl C61 butyric acid methyl (PCBM) hexagonal crystals grown by solvent-vapor annealing. Materials Chemistry and Physics, 2014, 145, 327-333.	2.0	13
158	Topological Phase Transition-Induced Triaxial Vector Magnetoresistance in (Bi <sub>1–<i>x</i></sub> In <sub><i>x</i></sub> ) <sub>2</sub> Se <sub>3</sub> Nanodevices. ACS Nano, 2018, 12, 1537-1543.	7.3	13
159	Thicknessâ€Dependent Asymmetric Potential Landscape and Polarization Relaxation in Ferroelectric Hf <i><sub>x</sub></i> Zr <sub>1â^'</sub> <i><sub>x</sub></i> O <sub>2</sub> Thin Films through Interfacial Bound Charges. Advanced Electronic Materials, 2019, 5, 1900554.	2.6	13
160	High-Performance CVD MoS <sub>2</sub> Transistors with Self-Aligned Top-Gate and Bi Contact. , 2021, , .		13
161	Reducing the power consumption of two-dimensional logic transistors. Journal of Semiconductors, 2019, 40, 091002.	2.0	12
162	Intercalation and hybrid heterostructure integration of two-dimensional atomic crystals with functional organic semiconductor molecules. Nano Research, 2020, 13, 2917-2924.	5.8	11

#	Article	IF	CITATIONS
163	Chemical stitching. Nature Nanotechnology, 2014, 9, 875-876.	15.6	10
164	Peculiar Magnetotransport Features of Ultranarrow Graphene Nanoribbons under High Magnetic Field. ACS Nano, 2016, 10, 1853-1858.	7.3	10
165	The effect of growth sequence on magnetization damping in Ta/CoFeB/MgO structures. Journal of Magnetism and Magnetic Materials, 2018, 450, 65-69.	1.0	10
166	Gate-tunable strong-weak localization transition in few-layer black phosphorus. Nanotechnology, 2018, 29, 035204.	1.3	10
167	Nonlinear resonant frequency of graphene/elastic/piezoelectric laminated films under active electric loading. International Journal of Mechanical Sciences, 2016, 115-116, 624-633.	3.6	9
168	Toward High-mobility and Low-power 2D MoS <inf>2</inf> Field-effect Transistors. , 2018, , .		9
169	Negative transconductance in multi-layer organic thin-film transistors. Nanotechnology, 2019, 30, 02LT01.	1.3	9
170	Molecular-Layer-Defined Asymmetric Schottky Contacts in Organic Planar Diodes for Self-Powered Optoelectronic Synapses. Journal of Physical Chemistry Letters, 2022, 13, 2338-2347.	2.1	9
171	A Smarter Pavlovian Dog with Optically Modulated Associative Learning in an Organic Ferroelectric Neuromem. Research, 2021, 2021, 9820502.	2.8	9
172	Sizeable Kane–Mele-like spin orbit coupling in graphene decorated with iridium clusters. Applied Physics Letters, 2016, 108, 203106.	1.5	8
173	Spin valley and giant quantum spin Hall gap of hydrofluorinated bismuth nanosheet. Scientific Reports, 2018, 8, 7436.	1.6	8
174	Observation of Strong <i>J</i> -Aggregate Light Emission in Monolayer Molecular Crystal on Hexagonal Boron Nitride. Journal of Physical Chemistry A, 2020, 124, 7340-7345.	1.1	8
175	Non-invasive digital etching of van der Waals semiconductors. Nature Communications, 2022, 13, 1844.	5.8	8
176	Enhanced opto-electrical properties of graphene electrode InGaN/GaN LEDs with a NiOx inter-layer. Solid-State Electronics, 2015, 109, 47-51.	0.8	7
177	The Unique Current-Direction Dependent On-Off Switching in BiSbTeSe <sub>2</sub> Topological Insulator Based Spin Valve Transistors. IEEE Electron Device Letters, 2016, , 1-1.	2.2	7
178	Electrical contacts to two-dimensional transition-metal dichalcogenides. Journal of Semiconductors, 2018, 39, 124001.	2.0	7
179	Probing Coulomb Interactions on Charge Transport in Few‣ayer Organic Crystalline Semiconductors by the Gated van der Pauw Method. Advanced Electronic Materials, 2020, 6, 2000136.	2.6	7
180	Layerâ€Defining Strategy to Grow Twoâ€Dimensional Molecular Crystals on a Liquid Surface down to the Monolayer Limit. Angewandte Chemie, 2019, 131, 16228-16232.	1.6	6

#	Article	IF	CITATIONS
181	Fluorinated graphene and hexagonal boron nitride as ALD seed layers for graphene-based van der Waals heterostructures. Nanotechnology, 2014, 25, 355202.	1.3	5
182	Patterning of self-assembled monolayers by phase-shifting mask and its applications in large-scale assembly of nanowires. Applied Physics Letters, 2015, 106, 041605.	1.5	5
183	Controlling relaxation dynamics of excitonic states in monolayer transition metal dichalcogenides WS2 through interface engineering. Applied Physics Letters, 2021, 118, 121104.	1.5	5
184	Reliability of Ultrathin High-Î $^{ m 2}$ Dielectrics on Chemical-vapor Deposited 2D Semiconductors. , 2020, , .		5
185	Width dependent edge distribution of graphene nanoribbons unzipped from multiwall carbon nanotubes. Journal of Applied Physics, 2013, 113, 174307.	1.1	4
186	Transition-metal dichalcogenides: Group-10 expands the spectrum. Science China: Physics, Mechanics and Astronomy, 2016, 59, 1.	2.0	3
187	2 step of conductance fluctuations due to the broken time-reversal symmetry in bulk-insulating BiSbTeSe2 devices. Applied Physics Letters, 2018, 112, .	1.5	3
188	A Compact Model for Transition Metal Dichalcogenide Field Effect Transistors with Effects of Interface Traps. , 2021, , .		3
189	Coulomb blockade effect of molecularly suspended graphene nanoribbons investigated with scanning tunneling microscopy. Physical Review B, 2013, 88, .	1.1	2
190	Electron transport and device physics in monolayer transition-metal dichalcogenides. , 2016, , .		2
191	A compact model for transition metal dichalcogenide field effect transistors with effects of interface traps. Science China Information Sciences, 2021, 64, 1.	2.7	2
192	Electrical contact properties between Yb and few-layer WS <sub>2</sub> . Applied Physics Letters, 2022, 120, 253505.	1.5	2
193	Enhancement of the ferroelectricity by interface engineering observed by in situ transmission electron microscope. Applied Physics Letters, 2022, 120, .	1.5	2
194	Preface to the Special Topic on 2D Materials and Devices. Journal of Semiconductors, 2017, 38, 031001.	2.0	1
195	Pressure Effect on Electronic and Excitonic Properties of Purely J-Aggregated Monolayer Organic Semiconductor. Journal of Physical Chemistry Letters, 2020, 11, 5896-5901.	2.1	1
196	Light-activated artificial synapses based on graphene hybrid phototransistors. , 2016, , .		1
197	Tunable terahertz radiation from graphene surface plasmon polaritons excited by parallel moving electron beam. , 2015, , .		0
198	Photoresist as a choice of molecularly thin gate dielectrics in graphene-based devices. APL Materials, 2021, 9, 031104.	2.2	0

#	Article	IF	CITATIONS
199	Reliability of Ultrathin High \$-mathcal{K}\$ Dielectrics on 2D Semiconductors. , 2021, , .		Ο
200	Photonic synaptic device capable of optical memory and logic operations. , 2017, , .		0
201	Aggregationâ€Dependent Dielectric Permittivity in 2D Molecular Crystals. Small Methods, 2022, , 2101198.	4.6	0
202	A nanogapped hysteresis-free field-effect transistor. Applied Physics Letters, 2022, 121, 023503.	1.5	0